

TEST ON 2-BAY 2-STORY CES FRAME SUBJECTED TO LATERAL LOAD REVERSALS

FAUZAN¹, Hiroshi KURAMOTO², Tomoya MATSUI³ and Takashi TAGUCHI⁴

¹ Postdoct. Researcher, Dept. of Architectural Engineering, Osaka University, Suita, Japan

² Professor, Dept. of Architectural Engineering, Osaka University, Suita, Japan

³ Assistance Prof., Dept. of Architecture and Civil Eng., Toyohashi Univ. of Technology, Toyohashi, Japan

⁴ Technical Research Institute for Earthquake Engineering, Yahagi Construction Co., Ltd.

Email: fauzan@arch.eng.osaka-u.ac.jp, kuramoto@arch.eng.osaka-u.ac.jp

ABSTRACT :

This paper summarizes the results of static loading test carried out on a two-bay two-story concrete encased steel (CES) frame. The structural members of the CES frame consist of only encased steel and fiber reinforcement concrete (FRC). The specimen was about a half-scale model, which simulated the lower 2.5 stories and 2 spans of the middle frame in 15-story CES frame buildings. It is predicted that the beam flexural failure near the interior beam-column joint occurred on the CES frame followed by the failure on all the bottom of columns. However, the failure on the joint panel of the interior beam-column joints also occurred at R of 0.01 rad. The specimen reached the maximum ultimate shear force at R of 0.02 rad. The results also showed that the use of FRC in the CES frame reduced the damage of the concrete in the frame. In addition, the hysteresis loops showed a stable behavior with almost no degradation of load carrying capacity until maximum story drift angle, R of 0.05 rad., indicating that the CES frame has excellent seismic behavior.

KEYWORDS: Composite structure, Fiber reinforced concrete (FRC), Frame, Seismic test

1. INTRODUCTION

Composite structural systems such as Steel Reinforced Concrete (SRC) and Concrete Filled Tube (CFT) structures have been widely used in high-rise and long-span buildings, especially in high seismic zone. Many types of new composite structure have been developed, and one of them is Concrete Encased Steel (CES) structural system that has been developed in recent 10 years (Kuramoto et al 2000, 2002, Shibayama et al. 2005, Nagata et al. 2006). The CES structural members such as beam and column consist of only steel and fiber reinforcement concrete (FRC). Some experimental and analytical studies have been carried for CES columns and CES beam-column joints to investigate its structural performance. For CES column, the encased steel covered by the precast FRC panel was proposed (Shibayama et al. 2005, Taguchi et al. 2006), in which the normal concrete was placed inside the panels, called PCa-CES construction method. In order to improve the structural behavior and composite action of the CES columns, the shear studs were used to connect the panel and the filled concrete. Under high applied axial force, it was found that the hysteresis characteristic of the columns was stable, even at large deformation. The results also indicated that the CES columns had excellent seismic performance which is almost similar or even more than those of the SRC columns. Similar results were also observed for CES interior and exterior beam-column joints that have been tested in recent year (Nagata et al. 2006, Matsui et al. 2007). The CES beam-column joints showed a stable hysteresis behavior and almost no concrete spalling was observed on the beam column joints even at large deformation.

Furthermore, a static loading test was carried on 2-bay 2-story CES frame to investigate its structural behavior. The main purpose of this study is to obtain the fundamental data which contributes to the development of seismic evaluation method for CES composite structural system. The behavior of the frame was examined in terms of hysteresis loop, failure mode, degree of damage and joint panel behavior. This paper summarizes and discusses the test results.

2. EXPERIMENTAL PROGRAM

2.1. Specimen

A 2-bay 2-span CES frame specimen was tested in this study. The specimen was about a half-scale model, which simulated the lower 2.5 stories and 2 spans of the middle frame in 15-story CES frame buildings. The dimensions and details of the specimen are shown in Fig. 1. The frame had columns with 400x400mm square sections and the story height of 2,000mm. The total height of frame from base floor to the top pin bearing was 4,800mm. The sections width and depth of the beams were 300x400mm with the span of 3,000mm. Built-in steels H-300×220×10×15 and H-300×150×6.5×9 were used to the columns and beams, respectively. The built-in steel continuous along the column height, while there was a bolt connection for built-in steel of beam at the position of 600mm from the column centers. Failure mechanism of the specimen supposed the entire collapse mechanism with beam flexural yieldings. Calculation results of maximum strength for columns, beams and joint panels are shown in Table 1. The strengths of the columns and beams were calculated using flexural analysis with superposition method, while the joint shear strength was calculated using AIJ standard for structural calculation of SRC structures (AIJ, 2001).

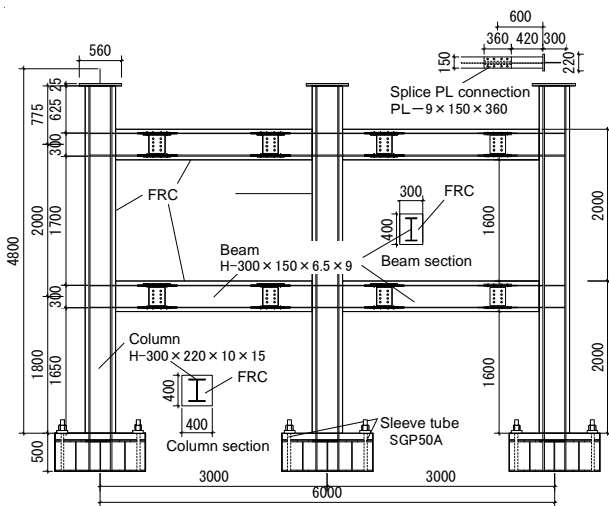


Figure 1 Test specimen

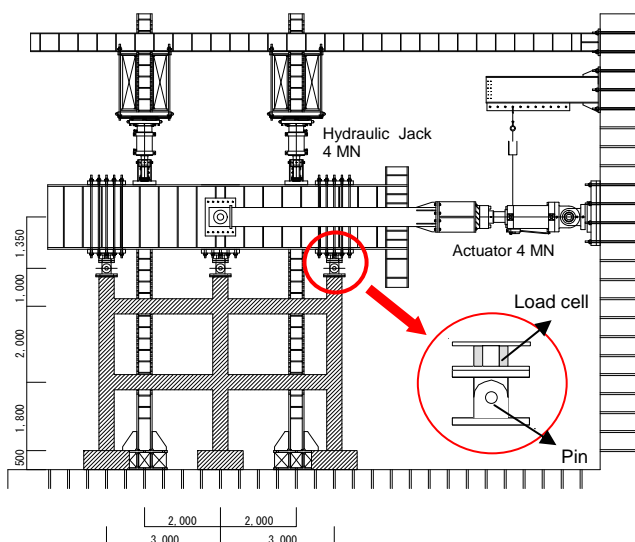


Figure 2 Schematic view of test setup

Table 1 Calculated strength

	Beam flexural strength [kNm]	Column Flexural strength [kNm]	Panel shear strength [kN]	Beam shear strength [kN]	Column shear strength [kN]
Interior column	238	622	399	534	799
Exterior column		608	333		

Table 2 Mechanical properties of FRC

	Type	Compressive strength [Mpa]	Tensile strength [Mpa]	Age [day]
1st Story	FRC	39.9	3.1	28
2nd Story		33.9	2.9	

Table 3 Mechanical properties of steel

	Type	Yield stress [Mpa]	Ultimate stress [Mpa]	Notes
H - 300x220 x10x15	SS400	320.8	452.1	Column flange
		361.0	476.6	Column web
315.6		483.1	Beam flange	
354.8		498.7	Beam web	

Table 4 FRC mix proportions

W/C (%)	Volume mixing ratio of fiber Vf (%)	water W (kg/m ³)	cement C (kg/m ³)	Sand S (kg/m ³)	Gravel G (kg/m ³)	Fiber Vf (kg/m ³)	Lime powder (kg/m ³)	Admixture (kg/m ³)
58	1.0	184	317	934	556	13	250	3.8

2.2. Material Used

The mechanical properties of FRC and the steel are given in Tables 2 and 3, respectively. In addition, the mechanical properties of concrete containing FRC are shown in Table 4. The type of fiber used in FRC was Polyvinyl Alcohol (PVA) fiber (RF 4000) with diameter of 0.66mm and length of 30mm. The placement of FRC was divided into 2 stages; the concrete was cast until 2nd floor beam first and then it was continued until the top of the frame.

2.3. Loading Method and Measurement

The specimen was connected to the loading devices through the pins which were installed in the inflection point of the 3rd story columns, as shown in Fig. 2. The applied axial force for the interior column was 1,920 kN (axial force ratio $(N/bD \sigma B = 0.3)$), while for the exterior columns were 1,620 kN ($N/bD \sigma B = 0.25$). The specimen was loaded by axial force and simultaneously loaded by lateral cyclic shear forces. The incremental loading cycles were controlled by average frame story drift angles, R , defined as the ratio of lateral displacements at the center of the 3rd floor interior beam-column joint, δ to the height of column from the base of column to the center of the 3rd floor beam, h (3,800mm). The lateral load sequence consisted of one cycles to each drift angle, R of 0.00125 and 0.0025 rads., followed by two cycle to each R of 0.005, 0.01, 0.015, 0.02 and 0.03 rads., and then half cycle to R of 0.05 rad.

In this experiment, the measurements of vertical and the horizontal direction loads, i.e. applied axial force and shear force were carried out by the load cells, which were installed on the top of 3rd floor columns (Fig. 2). Displacement at each story, deformations of beam-column joints, deformations of horizontal and axial directions in beams and columns were measured using the displacement transducers. The measurement of steel strain was carried out by installing the uniaxial strain gauges to the beam and column steels, and installing the three axial strain gauges to the joint panel of the beam-column joints.

3. EXPERIMENTAL RESULTS

3.1. Failure Characteristics

Failure modes of specimen after loading are shown in Fig. 3. At R of 0.00125 rad., flexural cracks occurred near all beam ends. These cracks increased at R of 0.005 rad., and there was almost no new crack occurred in the beams. At this stage, however, new cracks occurred in the base of column for each floor and on the side of the interior and exterior columns, which were vertical cracks (Fig. 3(i) and (j)). The shear cracks also occurred in the 3rd floor interior beam-column joint in this stage. At R of 0.01 rad., the cracks of the various parts of the beams and columns extended with the increase of story drift angle, and new shear cracks occurred in the 2nd floor interior beam-column joint. At R of 0.015rad., flexural cracks of beam almost didn't develop, however, cracks in various parts of the column significantly increased and concrete spalling was observed under the beam of the 3rd floor near beam-column joints. At R of 0.02 rad. cracks in various parts of the column increased and compression cracks was observed to all base of column sections in the 1st floor. At R of 0.03 rad., the cracks of the beam extended and shear cracks on interior beam-column joint of the 3rd floor significantly increased. In addition, the concrete spalling was observed in this stage.

In all beams, the flexural cracks developed at a position around 200 mm from the joint (Fig. 3(a) to (d)). For exterior beam-column joint with shear capacity magnification (SCM) factor of 2.24, almost no shear cracks occurred in the joint panel (Fig. 3(e) and (g)). However, the shear cracks in the joint panel was observed significantly in the interior beam-column joint (SCM factor = 1.34), which increased with the increase of drift angle (Fig. 3(f) and (h)). This indicates that the different SCM factor of beam-column joints resulted in different failure characteristics of the joints. For the column, furthermore, flexural cracks concentrated on the base of column at each floor. The compression failure of the column was clearly observed with the increase of the story drift angle (Fig. 3(k) and (l)).

Developments of maximum residual flexural cracks width of the beams and columns, and shear cracks width of the joint panels in 1st cycle of unloading stage for each drift angle are shown in Table 5. In the exterior

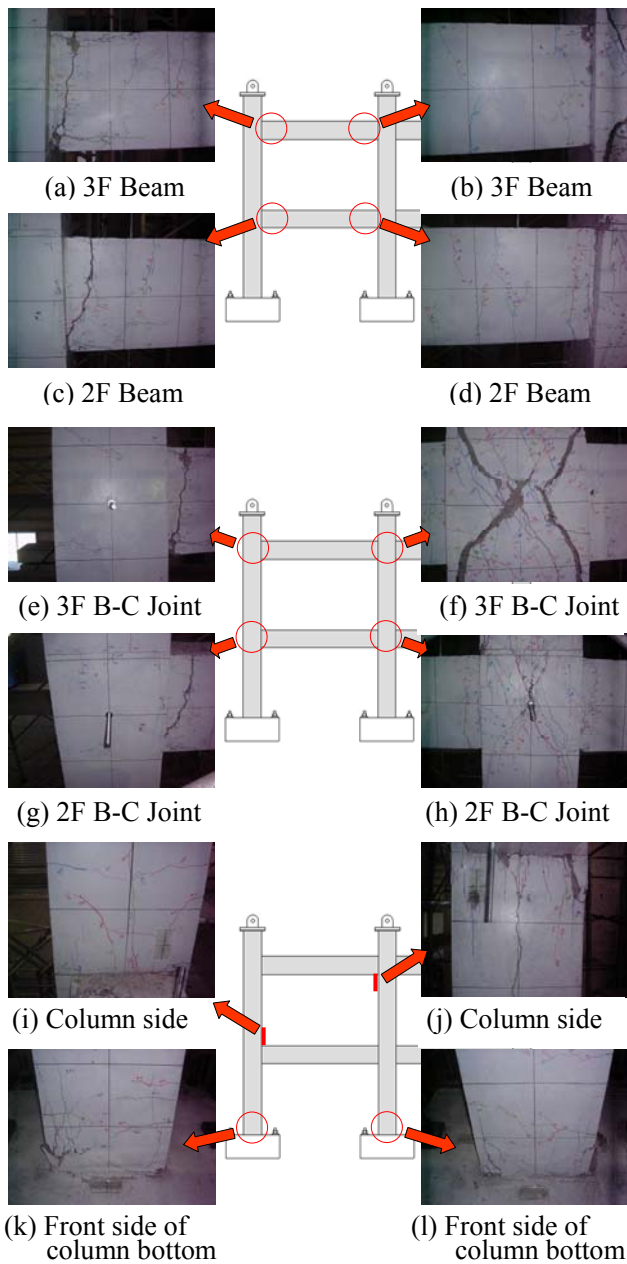


Figure 3 Crack modes at R of 0.05 rad.

beam-column joints, development of residual flexural crack width of the beam side end was observed significantly. The residual crack widths of the beams in the 3rd and 2nd floors at R of 0.03 rad. were 14mm and 8mm, respectively. In the interior joints, on the other hand, shear cracks occurred in the joint panel. The residual crack widths of interior joints in the 3rd and 2nd floors at R of 0.03 rad. were 22mm and 1mm, respectively. Both residual flexural and shear crack widths showed the tendency becoming large in the higher story.

3.2. Behavior of Structural Component

3.2.1 Behavior of beams

Until R of 0.0025 rad., the yielding of steel was not observed in all beams, which showed elastic behavior. At R of 0.005 rad., steel yielding was observed in the beam end flanges of the 3rd and 2nd floors near exterior joint, in the beam end flanges of the 3rd and 2nd floors near interior joint, and in the beam end web of the 3rd and 2nd floors near exterior joint. At R of 0.01 rad., moreover, the yielding of steel was observed in the beam end web of

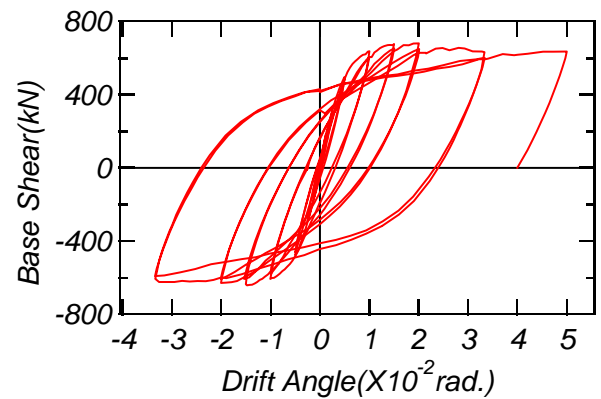


Figure 4 Shear versus average story drift angle relationships

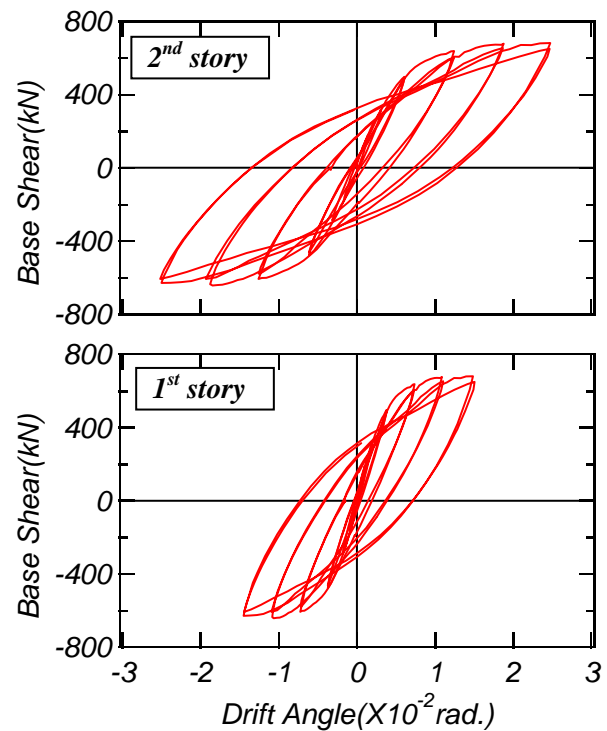


Figure 5 Shear versus drift angle relationships at each story frame

Table 5 Residual crack width

R [rad.]	Flexural cracks								Shear cracks	
	3F beam (near exterior column side) [mm]	2F beam (near exterior column side) [mm]	3F beam (near interior column side) [mm]	2F beam (near interior column side) [mm]	2F exterior column bottom [mm]	1F exterior column bottom [mm]	2F interior column bottom [mm]	1F interior column bottom [mm]	3F interior beam-column joint [mm]	2F interior beam- column joint [mm]
0.00125	0.05	0.02	0.08	0.04	-	-	-	-	-	-
0.0025	0.10	0.04	0.08	0.06	-	-	0.00	-	-	-
0.005	0.20	0.06	0.08	0.15	0.00	0.00	0.04	0.00	0.00	-
0.01	1.40	0.30	1.30	0.60	0.06	0.00	0.08	0.15	0.15	0.00
0.015	4.00	1.10	3.00	2.00	0.15	0.15	0.35	0.50	0.30	0.04
0.02	5.00	3.00	6.00	3.50	0.40	0.65	1.10	0.80	5.00	0.08
0.03	14.00	8.00	16.00	6.00	1.20	2.50	2.50	3.00	22.00	1.00

the 3rd and 2nd floors near interior joint. In addition, all beam end flanges and webs reached yielding at this point. Furthermore, it is confirmed that the yielding of steel web was initiated by the yielded of the steel flange.

3.2.2. Behavior of columns

Similar to the beams, the yielding of steel was not observed in the columns until R of 0.005 rad., which showed elastic behavior. At R of 0.01 rad., steel yielding was observed in the flange of the 2nd floor interior column bottom. At R of 0.015 rad., the yielding was observed in the flange and web of the 1st floor exterior column bottom, and in flange of the 1st floor interior column bottom. At R of 0.02 rad., yielding was observed in web of the 1st floor interior column bottom. In addition, steel flanges and webs in all columns bottom of the 1st floor also reached yielding in this stage.

3.2.3. Behavior of beam-column joints

Up to R of 0.005 rad., the yielding of the joint panel was not observed either in the joint panel, column flange or the stiffener, which showed elastic behavior. At R of 0.01 rad., the yielding occurred in the joint panel, column flange and stiffener of the 3rd and 2nd floors interior beam-column joints, and in the stiffener of the 3rd floor exterior beam-column joints. At R of 0.015 rad., there was no new yielding was observed in the joint panel, column flange and stiffener. At R of 0.02 rad., moreover, the yielding was observed on the stiffener of 2nd floor exterior beam-column joints. In this stage, all stiffeners were already yielded.

3.3. Hysteresis Characteristics

Base shear versus average story drift angle relationships of the specimen is shown in the Fig. 4. The based shear was calculated by summing the total of the shear forces which were measured on the top of the columns. The failure of specimen was initiated by yielding of the beam flange at R of 0.003 rad. The yielding of the beam increased at R of 0.01 rad., however, almost no strength degradation occurred in this stage. In positive loading, the specimen reached the maximum strength of 680.4 kN at R of 0.02 rad., while in negative loading, the maximum strength was reached at R of -0.015 rad with a base shear of -641.4 kN. The strength of the specimen in both positive and negative loading sides was almost kept constant until large drift angle, R of 0.05 rad. The strength of the specimen at last drift angle, R of 0.05 rad was 635.9 kN, which was approximately 90% of its maximum strength. From this figure, it can be seen that the CES frame specimen had a stable-spindle shaped hysteresis loops with large energy absorption, indicating that the specimen had excellent seismic performance.

Figure 5 showed the relationships between base shear versus 2nd story drift angle, R2 and between base shear versus 1st story drift angle, R1. The data used in this figure was measured until average story drift, R of 0.02 rad., where the maximum strength was reached. As seen in the figure, the deformation in the 2nd story was about 1.5 times that of in the 1st story due to the large development of residual cracks width in the 2nd story.

3.4. Damage Degree Evaluation of Structural Component

3.4.1. Summary of the degree of structural damage

Definition of the degree of damage for the structural component is shown in Fig. 6. The degree of damage for structural members mentioned in AIJ guidelines considering the scale of the structural repair which becomes necessary for damage circumstance and after the earthquake such as concrete which responds to limit state, residual cracks and compressive destruction, which is evaluated appropriately. The degree of damage was classified into 4 categories according to the limited state of the component, namely: degree of damage I (enable continue to use the structure), degree of damage II (easy to repair), degree of damage III (repairable) and degree of damage IV (maintain axial force limit). In this study, the degree of damage for each structural component of the frame such as columns, beams and beam-column joints, and the whole 2-bay 2-story CES frame was examined.

The degree of the damage mentioned in AIJ guidelines was used for evaluating the RC structures. However, it can also be used for the CES structures by replacing the reinforcing bar with the steel frame. In this study, stress intensity of steel frame, and concrete damage were evaluated on the basis of the maximum residual cracks width. In addition, the degree of damage for the whole 2-bay 2-story CES frame was evaluated based on the damage of each component and the base shear versus story drift angle relationships.

3.4.2. Evaluation results

The evaluation results of the damage degree for each component of the frame are shown in Table 6. For beam, degree of damage I was observed until R of 0.0025 rad., degree of damage II at R of 0.005 rad., degree of damage III at R of 0.01 rad. and degree of damage IV at R of 0.03 rad. For column, degree of damage I was observed at R of 0.01 rad., degree of damage II at R of 0.015 rad., degree of damage III at R of 0.02 rad., degree of damage IV at R of 0.03 rad. For the joint panel, degree of damage I was observed at R of 0.005 rad., degree of damage II at R of 0.015 rad., and degree of damage IV at R of 0.03 rad. For the whole 2-bay 2-story CES frame, on the other hand, degree of damage I was observed at R of 0.005 rad., degree of damage II at R of 0.01 rad., degree of damage III at R of 0.02 rad., and degree of damage IV at R of 0.03 rad. For 2-bay 2-story CES frame, each column has kept the respective axial force ratio of approximately 0.2 until R of 0.03 rad. At this stage, the strength reached 631 kN, which maintained approximately 90% of the maximum strength. This means that the degree of damage IV was maintained in large deformation that can be stated that it will not exceed the safety limit.

3.5. Behavior of Joint Panel

Figure 9 shows the base shear force versus joint distortion responses for joint panels (Fig. 8) until R of 0.03 rad. The joint distortion, γ_p , on the horizontal axes was calculated using Eqs. 3.1 and 3.2. Figure 7 shows the definition to calculate the joint distortion.

$$\gamma_p = \alpha_1 + \alpha_2 = \frac{\sqrt{h_p^2 + l_p^2}}{h_p \cdot l_p} x \quad (3.1)$$

$$\frac{x}{l_p} = \frac{\delta_1 + \delta_1' + \delta_2 + \delta_2'}{2} \quad (3.2)$$

where h_p , l_p and δ_1 , δ_1' , δ_2 , δ_2' are shown in Fig. 8.

As seen in this figure, the joint distortions of exterior beam-column joints in the 3rd and 2nd floors were relatively small until R of 0.003 rad. In the interior beam-column joints, however, the joint distortions of the 3rd and 2nd floor reached around 0.03 rad. and 0.015 rad., respectively. The different SCM factor between exterior beam-column joints (2.24) and interior beam-column joints (1.34) clearly recognized the difference of joint distortion in the joint panels. For the same SCM factor, moreover, the joint distortion of the interior beam-column joint in the 3rd floor was approximately 2 times that of in the 2nd floor, indicating that the joint distortion increased in the higher story of the frame.

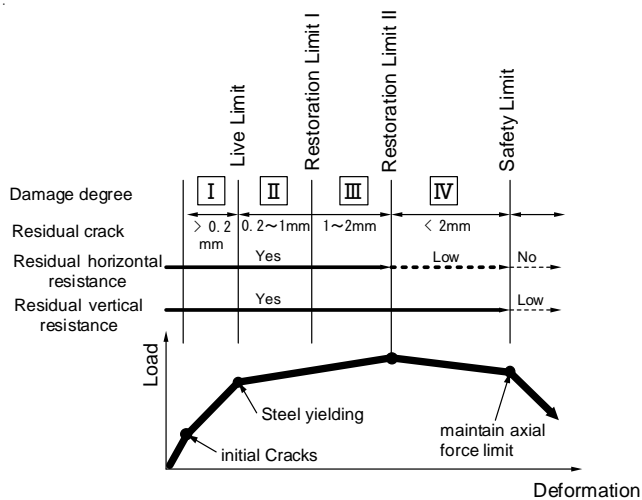


Figure 6 Schematic degree of damage (AIJ)

Table 6 Results of damage evaluation

R [rad.]	Beam	Column	Beam-column joint	Frame
0.00125	I	I	I	I
0.0025	I	I	I	I
0.005	II	I	I	I
0.01	III	I	II	II
0.015	IV	II	II	III
0.02	IV	III	IV	III
0.03	IV	IV	IV	IV

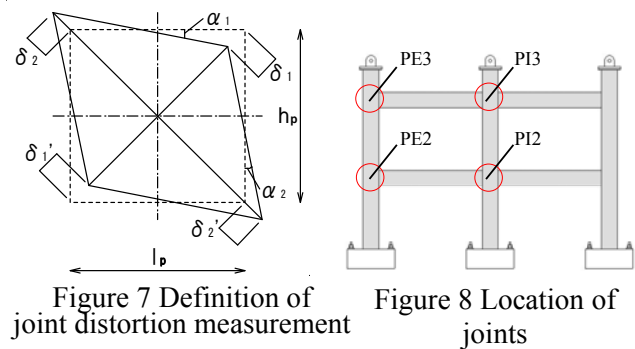


Figure 7 Definition of joint distortion measurement

Figure 8 Location of joints

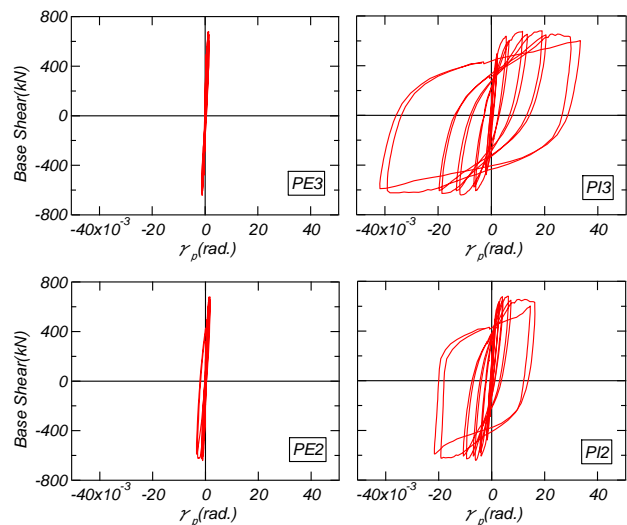


Figure 9 Joint distortions of beam-column joints

Figure 10 shows the contributions of deformation by the column, beam, and joint panel to the total deformation of the joint panels for all beam-column joints of the frame until R of 0.02 rad. The values were obtained by measuring the deformations of beam, column and panel zone from transducers installed on the steels of each component (Fig. 12). The deformations of the column and the joint panel were converted into the deformation of beam, as described in Fig. 11. In interior beam-column joint of the 3rd floor, the deformation ratio of the beam decreased with the increase of drift angle and it fluctuated in the 2nd floor, while deformation ratio of the column was almost constant in the 3rd floor at approximately 10 % and slightly decreased in the 2nd floor. In panel zone, moreover, the deformation ratio of the joint panel increased in the 3rd floor, while it keeps constant at approximately 15% in the 2nd floor. In exterior beam-column joints, the deformation ratio of the beam in both stories increased significantly with the increase of drift angle, while the deformation ratio of the column and joint panel decreased. By comparing the interior and exterior beam-column joints, there was a tendency where deformation ratio of the interior joint panel becomes large due to the influence of SCM factor.

4. CONCLUSIONS

In this study, static loading experiment was carried out on a 2-bay 2-story CES frame. The following conclusions can be drawn:

1. The use of FRC in CES frame reduced the damage of the beam-column joints. The spalling of concrete was not observed on the frame even at large drift angle, R of 0.03 rad.
2. The 2-bay 2-story CES frame had a stable-spindle shaped hysteresis loops with large energy absorption capacity. The strength of the frame was approximately 90% of its maximum strength at large R of 0.05 rad. This indicates that the structure had an excellent seismic performance.

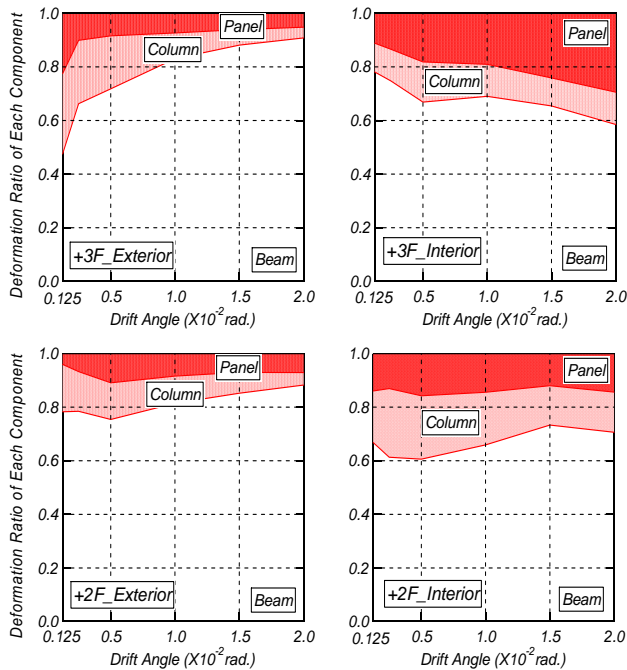


Figure 10 Deformation ratio of each component

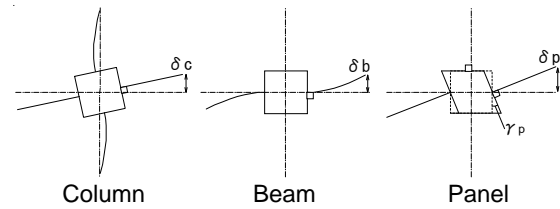


Figure 11 Definition of joint deformation of each component

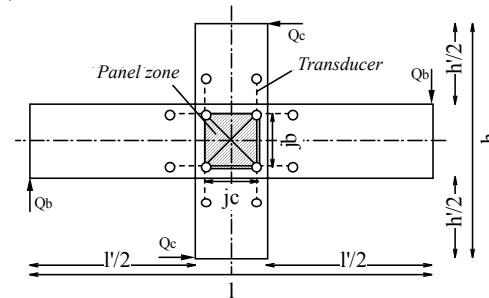


Figure 12 Definition of shear force in panel zone

3. The CES frame maintained the axial force limit, where the strength was kept stable around the maximum capacity until large deformation, R of 0.05 rad. indicating that the frame is within the safety limit.
4. In the exterior beam-column joints which had high shear capacity magnification (SCM) factor, the beam flexural failure was observed, while deformation of the joint panel was not verified.
5. In the interior beam-column joint which had a small SCM factor, the deformation of the joint panel increased with the increase of drift angle. The yielding of the joint panel occurred in the 3rd and 2nd floors of the interior joints, where the significant yielding was observed clearly in the higher story of the frame.

REFERENCES

- Architectural Institute of Japan (2001). AIJ Standard for Structural Calculation of Steel Reinforced Concrete Structures. AIJ, Tokyo, Japan.
- Architectural Institute of Japan, Seismic Performance Evaluation Guidelines of RC structures, AIJ, Tokyo, Japan (under publishing process).
- Kuramoto, H., Takahashi, H. and Maeda, M. (2000). Feasibility study on structural performance of concrete encased steel columns using high performance fiber reinforced cementitious composites. *Summaries of Technical Papers of Annual Meeting, AIJ, Vol.C-1*, 1085–1088.
- Kuramoto, H., Adachi, T. and Kawasaki, K. (2002). Behavior of concrete encased steel composite columns using FRC. *Proceedings of Workshop on Smart Structural Systems Organized for US-Japan Cooperative Research Programs on Smart Structural Systems (Auto-Adaptive Media) and Urban Earthquake Disaster Mitigation*, Tsukuba, Japan, 13-26.
- Nagata, S., Matsui, T. and Kuramoto, H. (2006). A fundamental study on structural performance of CES beam-column joints. *Proceedings of the Japan Concrete Institute Vol.28 (2)*, 1279-1284.
- Matsui, T., Iwase, K., Nagata, S., and Kuramoto, H. (2007). A fundamental study on structural performance of CES exterior beam-column joints. *Summaries of Technical Papers of Annual Meeting, AIJ, Vol.C-1*, 1261–1264.
- Shibayama, Y. and Kuramoto, H. (2005). A study on restoring force characteristic of CES columns covered by FRC panels. *Proceedings of the Japan Concrete Institute Vol.27 (2)*, 241-246.
- Taguchi, T., Nagata, S., Matsui, T. and Kuramoto, H. (2006). Structural Performance of CES Columns encased H-section steel. *Proceeding of the Japan Concrete Institute Vol.28 (2)*, 1273-1278.